

# Geophysical Research Letters

## RESEARCH LETTER

10.1029/2021GL094204

### Special Section:

The COVID-19 pandemic: linking health, society and environment

### Key Points:

- The ozone concentration in the northern extratropical free troposphere was 5%–15% lower in May and June 2020 relative to climatology
- A third of this anomaly is attributed to meteorological conditions including stratospheric Arctic air with abnormally low ozone
- The assumed reduction in surface and aircraft emissions associated with the COVID-19 pandemic can explain an ozone anomaly of 4%–8%

### Supporting Information:

Supporting Information may be found in the online version of this article.

### Correspondence to:

G. P. Brasseur,  
[guy.brasseur@mpimet.mpg.de](mailto:guy.brasseur@mpimet.mpg.de)

### Citation:

Bouarar, I., Gaubert, B., Brasseur, G. P., Steinbrecht, W., Doumbia, T., Tilmes, S., et al. (2021). Ozone anomalies in the free troposphere during the COVID-19 pandemic. *Geophysical Research Letters*, 48, e2021GL094204. <https://doi.org/10.1029/2021GL094204>

Received 8 MAY 2021

Accepted 3 AUG 2021

### Author Contributions:


**Conceptualization:** Idir Bouarar, Benjamin Gaubert, Guy P. Brasseur, Wolfgang Steinbrecht

**Formal analysis:** Idir Bouarar, Benjamin Gaubert, Guy P. Brasseur, Wolfgang Steinbrecht, Thierno Doumbia, Trisisevgeni Stavrakou,

© 2021. The Authors.

This is an open access article under the terms of the [Creative Commons Attribution-NonCommercial License](#), which permits use, distribution and reproduction in any medium, provided the original work is properly cited and is not used for commercial purposes.

## Ozone Anomalies in the Free Troposphere During the COVID-19 Pandemic

Idir Bouarar<sup>1</sup>, Benjamin Gaubert<sup>2</sup> , Guy P. Brasseur<sup>1,2,3</sup> , Wolfgang Steinbrecht<sup>4</sup> , Thierno Doumbia<sup>5</sup>, Simone Tilmes<sup>2</sup> , Yiming Liu<sup>6</sup>, Trisisevgeni Stavrakou<sup>7</sup> , Adrien Deroubaix<sup>1</sup> , Sabine Darras<sup>8</sup>, Claire Granier<sup>5,9</sup>, Forrest Lacey<sup>2</sup> , Jean-François Müller<sup>7</sup> , Xiaoqin Shi<sup>1</sup> , Nellie Elguindi<sup>5</sup> , and Tao Wang<sup>3</sup>

<sup>1</sup>Environmental Modeling Group, Max Planck Institute for Meteorology, Hamburg, Germany, <sup>2</sup>Atmospheric Chemistry Observations and Modeling Laboratory, National Center for Atmospheric Research, Boulder, CO, USA, <sup>3</sup>Department of Civil and Environmental Engineering, The Hong Kong Polytechnic University, Hong Kong, China, <sup>4</sup>Deutscher Wetterdienst, Hohenpeißenberg, Germany, <sup>5</sup>Laboratoire d'Aérodynamique, Université de Toulouse, CNRS, UPS, Toulouse, France, <sup>6</sup>School of Atmospheric Science, Sun Yat-sen University, Guangzhou, China, <sup>7</sup>Royal Belgian Institute for Space Aeronomy, Brussels, Belgium, <sup>8</sup>Observatoire Midi-Pyrénées, Toulouse, France, <sup>9</sup>NOAA Chemical Sciences Laboratory/CIRES, University of Colorado, Boulder, CO, USA

**Abstract** Using the CAM-chem Model, we simulate the response of chemical species in the free troposphere to scenarios of primary pollutant emission reductions during the COVID-19 pandemic. Zonally averaged ozone in the free troposphere during Northern Hemisphere spring and summer is found to be 5%–15% lower than 19-yr climatological values, in good agreement with observations. About one third of this anomaly is attributed to the reduction scenario of air traffic during the pandemic, another third to the reduction scenario of surface emissions, the remainder to 2020 meteorological conditions, including the exceptional springtime Arctic stratospheric ozone depletion. For the combined emission reductions, the overall COVID-19 reduction in northern hemisphere tropospheric ozone in June is less than 5 ppb below 400 hPa, but reaches 8 ppb at 250 hPa. In the Southern Hemisphere, COVID-19 related ozone reductions by 4%–6% were masked by comparable ozone increases due to other changes in 2020.

**Plain Language Summary** The reduction in the emissions of primary air pollutants during the 2020 COVID-19 pandemic has generated perturbations in the chemical state of the atmosphere. A global Earth system model that accounts for chemical, physical, and dynamical processes in the atmosphere and for the coupling between the atmosphere, the ocean and the land surface, indicates that the abundance of tropospheric ozone was significantly reduced during the pandemic in response to realistic scenarios of reduced emissions of primary pollutants associated with restrictions of air traffic and economic activities. These simulated findings are consistent with observed ozone anomalies during the summer of 2020.

## 1. Introduction

The reduction in the emissions of primary pollutants during the COVID-19 pandemic, due to the worldwide slowdown in economic activity, produced a perturbation in the formation of secondary compounds, including ozone, and in the oxidative capacity of the lower atmosphere. Several studies have highlighted that the sign and magnitude of the anomaly depended on the photochemical regime in the region under consideration (Cazorla et al., 2020; Gaubert et al., 2021; Le et al., 2020; Miyazaki et al., 2020; Venter et al., 2020;). In China, for example, where a strict lockdown was imposed as early as January 2020, the surface concentration of ozone increased in the North China Plain and in the major cities of the country (Gaubert et al., 2021; Huang et al., 2020; Liu et al., 2021; Miyazaki et al., 2020; Shi & Brasseur, 2020). In these NO<sub>x</sub> saturated regions, the titration of ozone by nitrogen oxides was reduced during the entire lockdown period. In contrast, in the rural areas of southern China, which are NO<sub>x</sub>-controlled, the surface concentration of ozone decreased during the pandemic (Lian et al., 2020; Liu et al., 2021). In the rest of the world, where the most stringent containment measures were introduced only in March and April 2020, the concentrations of surface ozone in remote areas were generally reduced (Gaubert et al., 2021; Weber et al., 2020) with positive anomalies mostly driven by meteorological conditions (Deroubaix et al., 2021; Ordóñez et al., 2020).

Adrien Deroubaix, Sabine Darras, Claire Granier, Forrest Lacey, Jean-François Müller, Xiaoqin Shi, Nellie Elguindi, Tao Wang

**Methodology:** Benjamin Gaubert, Simone Tilmes

**Writing – original draft:** Benjamin Gaubert, Guy P. Brasseur, Wolfgang Steinbrecht

**Writing – review & editing:** Idir Bouarar, Benjamin Gaubert, Guy P. Brasseur, Wolfgang Steinbrecht, Thierno Doumbia, Simone Tilmes, Yiming Liu, Trisseyeni Stavrakou, Adrien Deroubaix, Sabine Darras, Claire Granier, Forrest Lacey, Jean-François Müller, Xiaoqin Shi, Nellie Elguindi, Tao Wang

Most of the early data analyses about the effect of the pandemic on air quality have focused on chemical species anomalies at the Earth's surface and were based on measurements from monitoring stations (Huang et al., 2020; Shi & Brasseur, 2020) and, for a limited number of species (e.g., nitrogen dioxide), on information deduced from satellite observations (e.g., the Tropospheric Monitoring Instrument; Bauwens et al., 2020). Little information on the effects of the chemical perturbations during the COVID-19 pandemic in the free troposphere is currently available. A recent study (Steinbrecht et al., 2021) based on ozone measurements by balloon-borne ozone sondes as well as ground-based FTIR and LIDAR systems during the period 2000–2020 at latitudes 82.5°N–54.5°S reported changes of free tropospheric ozone related to the COVID-19 disruptions. It shows that, from April to August 2020 and from 1 to 8 km altitude, the average concentration of ozone was 7% lower than the climatological mean values across most of the Northern Hemisphere.

To help interpret the reduced ozone concentrations, we use the global Community Atmosphere Model with chemistry (CAM-chem) and, assuming a few emission reduction scenarios, quantify the relative importance of the different processes that have contributed to the observed ozone anomalies. Unlike the situation in the boundary layer where the lifetime of ozone is of the order of a few days (Goldberg et al., 2015), the timescales associated with the temporal evolution of odd oxygen ( $O_x = O_3 + NO_2$ ) in the free troposphere are of the order of several weeks (Stevenson et al., 2006), or even several months (Bates & Jacob, 2020) if one includes hydrogenated compounds ( $HO_x$  and its chemical reservoirs) in the definition of  $O_x$ . The behavior of ozone in the free troposphere therefore depends both on photochemical processes and on the effect of transport due to the atmospheric circulation.

During the year 2020, several events potentially affected ozone in the free troposphere: (a) the intense world-wide disruption of the surface emissions of primary pollutants in response to the COVID-19 pandemic; (b) the related reduction in air traffic with a reduced injection of  $NO_x$ ,  $SO_2$ , and black carbon (BC) into the upper troposphere; (c) the particularly intense depletion of ozone in the lower Arctic stratosphere due to the abnormally stable and vigorous polar vortex during the first months of 2020 (Inness et al., 2020; Manney et al., 2020; Wilka et al., 2021; Wohltmann et al., 2020), (d) the interannual variability associated with meteorology, lightning and fires. The perturbation in air traffic during the COVID-19 pandemic has also modified the density of aircraft-generated contrails and cirrus clouds (Schumann et al., 2021).

Here, we estimate the response of free tropospheric ozone to the aforementioned potential causes of the 2020 ozone anomaly by performing several sensitivity simulations in which the different sources of disturbances are taken into account. We compare the simulated overall responses with observed ozone anomalies from Steinbrecht et al. (2021).

## 2. Model Description and Overview of Simulations

We use the Community Earth System Model (CESM) version 2.2 (Danabasoglu et al., 2020; Gaubert, Emmons, et al., 2020; Gaubert, Tilmes, et al., 2020; Gettelman et al., 2019; Tilmes et al., 2020), described and evaluated in Gaubert et al. (2021). We adopt the MOZART Troposphere Stratosphere (TS1) chemistry mechanism (Emmons et al., 2020), which includes 221 gas phase and aerosol species and 528 chemical and photochemical reactions. Aerosol concentrations and size distribution are derived from the four-mode Modal Aerosol Model (MAM4, Liu et al., 2016; Mills et al., 2016). In order to realistically represent meteorological conditions for the period under consideration, the wind velocity components and the temperature are nudged toward the MERRA-2 meteorological analysis (Gelaro et al., 2017). Figure S1 shows the calculated zonally mean of  $NO_x$  and ozone concentrations averaged over the month of 2020 (baseline case = control).

Baseline anthropogenic surface emissions rely on the Copernicus Atmosphere Monitoring Service (CAMS)-GLOB-ANT\_v4.2-R1.1 global inventory (Elguindi et al., 2020; Granier et al., 2019). Three-dimensional aircraft emissions are based on Hoesly et al. (2018). Biogenic emissions are calculated online from the Model of Emissions of Gases and Aerosols from Nature (Guenther et al., 2012). Daily biomass burning emissions are based the Quick-Fire Emissions Dataset (Darmanov & da Silva, 2014) include, for example, the 2019/2020 large fires in California, Colorado, and Australia. Deposition of gases and aerosols are calculated through an active coupling between the atmosphere and the Community Land Model version 5 (Lawrence et al., 2019). To account for the effect of the COVID-19 lockdowns, we follow the emission reductions

estimated in Doumbia et al. (2021). Anthropogenic emissions are reduced for each economic activity sector (industrial, mobility, residential, energy, shipping, and aviation) and geographical region according to the central best estimate of the CONFORM dataset (Doumbia et al., 2021, see also Figure S2). The emission reductions adopted in other studies (Lamboll et al., 2021; Mertens et al., 2021; Miyazaki et al., 2021; Weber et al., 2020) can be rather different, which highlights the substantial uncertainties in these estimates. The uncertainties estimated by Doumbia et al. (2021) for different sectors in different regions of the world are provided in Table S1. Globally, the uncertainties range from  $\pm 12\%$  to  $\pm 25\%$ . Nevertheless, the different model simulations performed for the present study (summarized in Table S2), as well as results similar to ours obtained in the studies of Weber et al. (2020), Miyazaki et al. (2021), and Mertens et al. (2021), indicate that the responses in the free troposphere depend more or less linearly on the chosen reduction scenarios and their magnitude. Two specific uncertainties, which have a large influence on the ozone response in the middle to the upper troposphere are assessed explicitly here: (a) the calculated springtime ozone depletion in the Arctic, which is a strong function of the adopted denitrification rate inside the polar vortex and (b) the reduction in air traffic during the pandemic.

We first present the calculated anomalies in the concentration of chemical species in the troposphere during year 2020 relative to a baseline case in which the COVID-related changes in the emissions are ignored. These numerical experiments only quantify changes due to the anthropogenic emissions following lockdowns across the world. We consider three scenarios: changes only in the surface emissions during the pandemic (Case 1 = COVID-surf – Control); changes only in the air traffic emissions (Case 2 = COVID-airc – Control) and the combined effects (Case 3 = COVID-ALL – Control). We focus on the monthly mean changes in the global distribution of  $\text{NO}_x$  and ozone in a global domain extending from the surface to the lower stratosphere and from pole to pole. We then assess the contribution of meteorological inter-annual atmospheric variability, including the influence of the exceptionally high ozone depletion inside the 2020 Arctic vortex, by comparing the baseline 2020 results (no COVID related effects included) with 2001–2019 climatology (Case 4 = Control – CLIMO). Finally, we perform a comparison similar to Case 4, but with the year 2020 simulation accounting also for the reduced anthropogenic emissions during the pandemic (Case 5 = COVID-ALL – CLIMO). This last case can be compared with the results of Steinbrecht et al. (2021), in which observed ozone concentrations in 2020 are contrasted to the observed ozone climatology. In Case 6 (=COVID-ALL-W – CLIMO), we assess how higher denitrification rate in the polar vortex, which affects the intensity of the springtime Arctic stratospheric ozone depletion, also increases the calculated tropospheric ozone anomaly in 2020. Case 7 (=COVID-ALL2 – Control) assesses the sensitivity of the calculated ozone perturbation to the magnitude of the reduction in aircraft emissions. This case is similar to Case 3 (=COVID-ALL – Control), but with the COVID-19 adjustment in aircraft emissions reduced by one-third.

### 3. Results

Figure 1 shows the response of the zonally and monthly averaged ozone concentration to the perturbed emissions (Case 3 = COVID-ALL – Control) relative to the baseline case in which no lockdown effect is applied to the emissions. We note the gradually larger reduction in the ozone concentration as time proceeds and photochemical activity increases; the relative anomaly does not exceed 2% in March, but reaches 7% in May and June before it slightly decreases in July (panels a–f of Figure 1). While the lockdown measures were stricter in the Northern Hemisphere winter and spring 2020, the photochemical response of ozone was largest in summer. The relative changes in the concentration are more pronounced in the lower to middle troposphere (800–300 hPa, or 2–9 km altitude), but the absolute changes (up to 8 ppbv in June, see Figure 1, panels g–i) are largest at higher altitudes (between 300 and 200 hPa or 9 and 12 km, respectively) in the extratropics of the Northern Hemisphere. For Case 7, in which the reduction in air traffic emissions is one third smaller than in Case 3, the maximum absolute ozone depletion (ppbv) located near 300 hPa in the northern extratropics is smaller by about 1–2 ppbv (roughly 30% less) during the May–July 2020 period (panels j–l of Figure 1). When examining the relative changes, we also note that the location of the maximum response evolves with latitude following the mean solar radiation. The largest response occurs first in the tropics (March and April) with a gradual displacement toward the northern polar region (May–July).

We now investigate the contribution of the different forcing factors to the calculated ozone anomaly. We focus on June 2020 during which the ozone reduction is largest. In Figure 2, we show the response of zonal

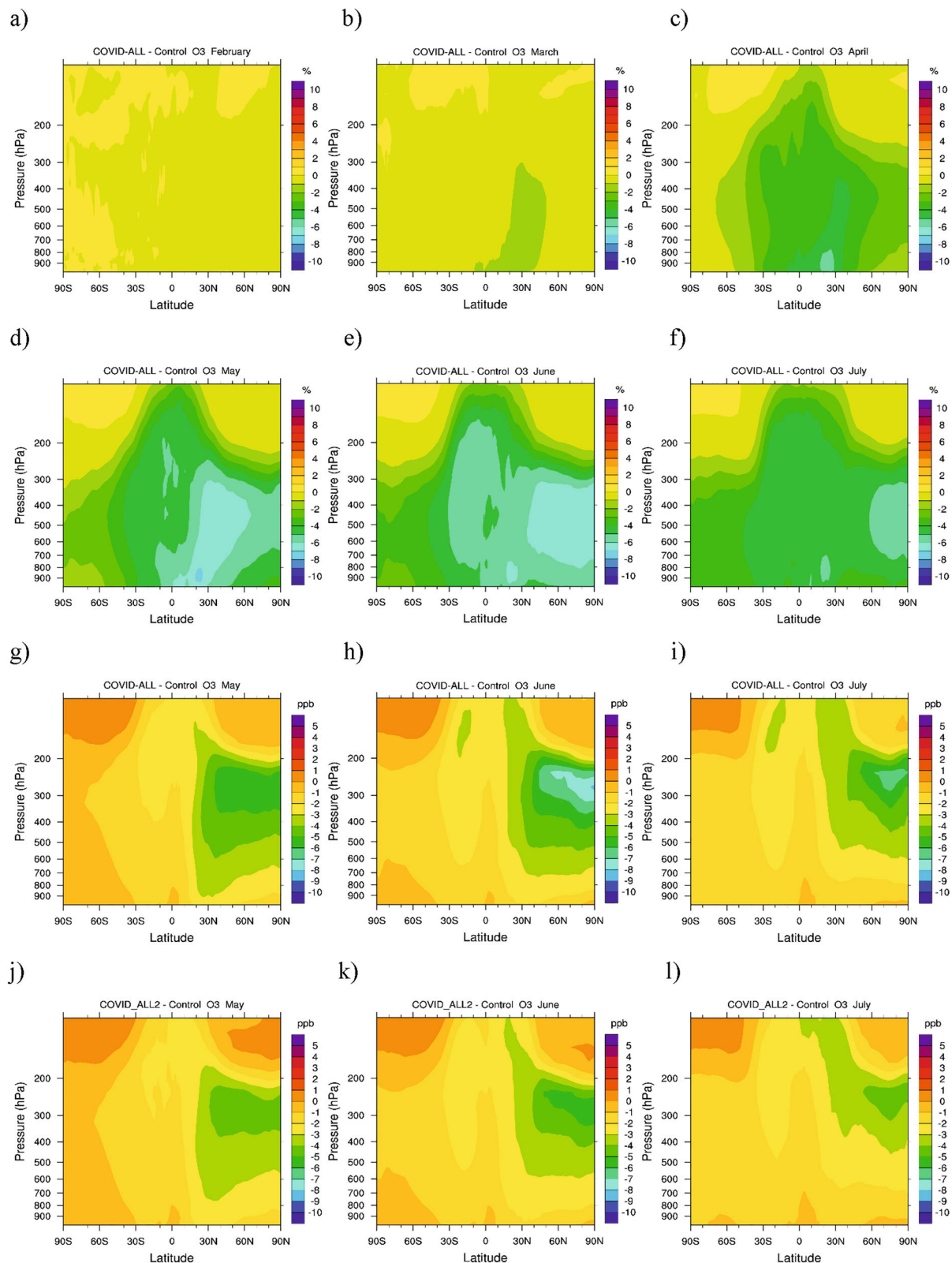


**Figure 1.** Change in the zonally and monthly averaged ozone mixing ratio between the surface and the upper troposphere for different months in response to the combined changes in the emissions of pollutants during the COVID-19 pandemic (Case 3 = COVID-ALL – Control). Panels a–f show relative changes from February to July 2020 (%). Panels g–i show similar results but in absolute terms (ppbv) for the period of May–July 2020. Panels j–l show the same, but with the COVID-19 related adjustment in air traffic reduced by one third (Case 7 = COVID-ALL2 – Control).



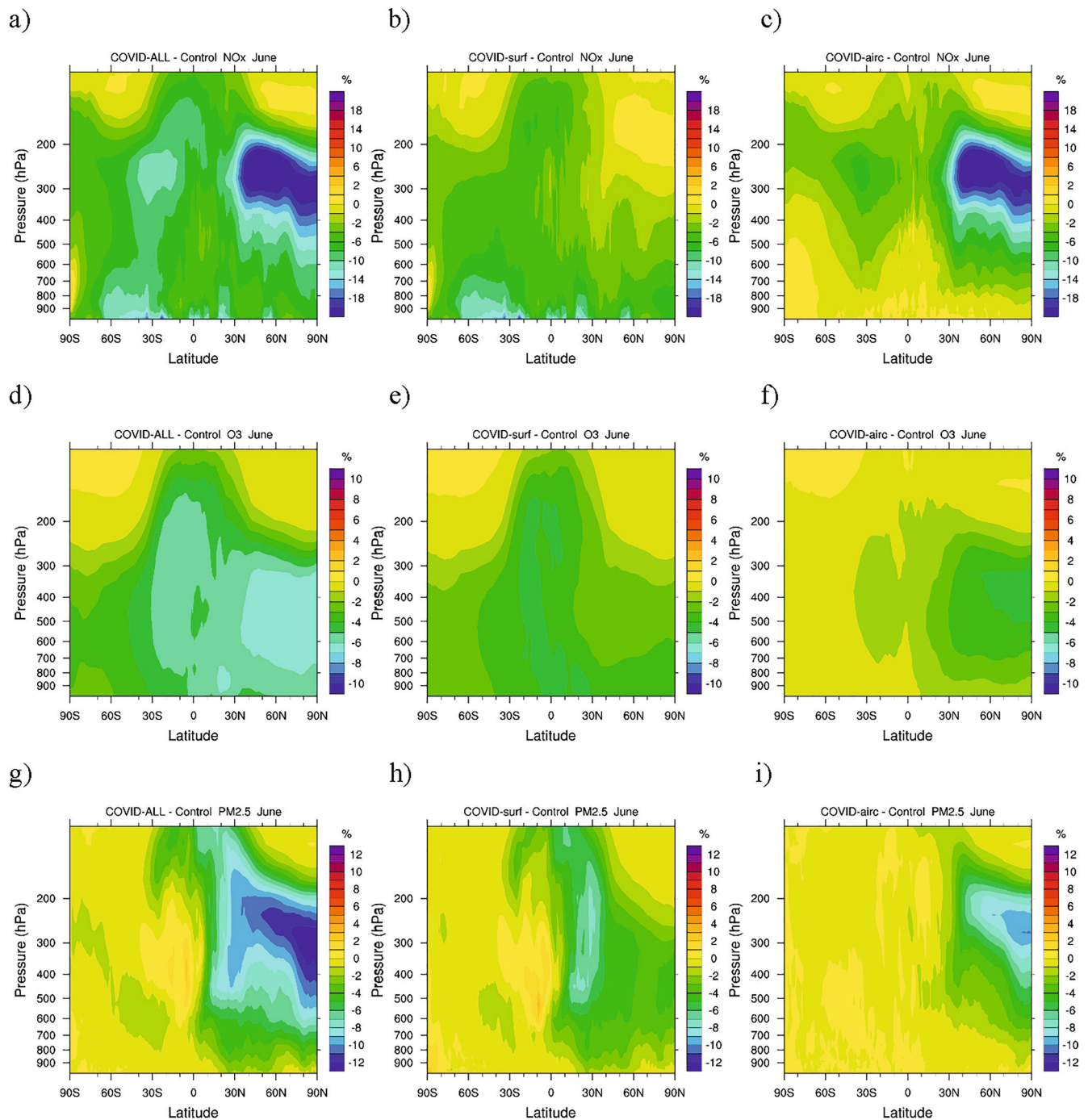


**Figure 2.** Change from the surface to the lower stratosphere in the zonally and monthly averaged concentration of  $\text{NO}_x$  (%), ozone (%), and  $\text{PM}_{2.5}$  (%) in June 2020 relative to a baseline case in which the COVID-19 related changes in the emissions or primary species are ignored. Left: response to changes in surface and air traffic emissions (Case 3 = COVID-ALL – Control); Middle: response to changes in surface emissions only (Case 1 = COVID-surf – Control); Right: response to the reduction in aircraft emissions (Case 2 = COVID-airc – Control).

and monthly mean concentrations of  $\text{NO}_x$  (panels a–c), ozone (panels d–f) and particulate matter ( $\text{PM}_{2.5}$ , panels g–i) to the changes in surface emissions (middle panels, Case 1 = COVID-surf – Control) and aircraft emissions (right panels, Case 2 = COVID-airc – Control), and to the combined changes (left panels, Case 3 = COVID-ALL – Control). In the case of  $\text{NO}_x$ , the response to the reduced surface emissions (Case 1 = COVID-surf – Control) is generally largest in the planetary boundary layer (larger than 10%), except

in the tropics where  $\text{NO}_x$ -depleted near-surface air masses are lifted to the upper troposphere by convective transport resulting in 5%–8% reductions in the concentrations. The effect of tropical convection is also visible in the case of ozone (reduction of 3%–4%) and  $\text{PM}_{2.5}$  (reduction of 5%–8%).

Large concentration changes resulting from the dramatic reduction in air traffic during the pandemic (Case 2 = COVID-airc – Control) are derived by the model. Between 300 and 200 hPa (9 and 12 km), the zonal and monthly mean  $\text{NO}_x$  concentration is reduced by more than 20% north of 30°N, while that of ozone is reduced by 4%–5% north of 60°N. Because of the increase with altitude of the background ozone concentration, the maximum ozone depletion in relative terms is located near 400 hPa (7 km), while in absolute terms (reduction of 7 ppbv), it is located higher in the atmosphere near 250 hPa (10 km). A secondary maximum decrease in the  $\text{NO}_x$  concentration of 7% is found near 30°S. The reduction in  $\text{PM}_{2.5}$  associated with reduced air traffic reaches 15% near 300 hPa and results from a reduction of similar magnitude in the concentration of sulfate and BC particles.

The zonally averaged perturbations in June, resulting from the combined changes in surface and aircraft emissions during the pandemic relative to the baseline simulation (Case 3 = COVID-ALL – Control), are shown by the left panels of Figure 2. Note that combined changes (in the left panels) are comparable to the sum of the individual changes (sum of middle and right panel). For ozone and  $\text{NO}_x$ , the overall response in the free troposphere depends fairly linearly on the emission reduction scenarios. In the specific case of  $\text{NO}_x$  (panel a), for the chosen scenario, the relative reduction in the concentration is higher than 10% in the boundary layer at several latitudes and in the upper troposphere north of 30°N and between 40°S and 15°S. In the case of ozone (panel d), the calculated reduction in June reaches 6%–7% north of 30°N between 800 and 300 hPa (2 and 9 km). The reduction is close to 5% in the tropics (30°S–30°N) and extends up to the tropopause. Vertical profiles of the changes in the monthly and zonally mean ozone reductions (in ppbv) relative to the baseline simulation and calculated poleward of 65°S in the tropics and poleward of 65°N are shown in Figure S3.

#### 4. Effects of 2020 Meteorological Conditions and Comparison With Observations

The interannual variations in the strength of the stratospheric circulation and dynamical variability impact the tropospheric ozone burden (Archibald et al., 2020). Specifically, deep intrusions of stratospheric ozone frequently reach the middle and even lower troposphere at midlatitudes during winter and spring, and can contribute significantly to ozone variability in the troposphere (Terao et al., 2008). This meteorologically induced variability (Case 4 = Control – CLIMO) needs to be accounted for, for example, when comparing our simulations with observed changes (Case 5 = COVID-ALL – CLIMO). Particularly in 2020, early and persistent cold conditions led to an exceptionally stable polar vortex and to record-low ozone in the Arctic, as highlighted by MLS observations (Manney et al., 2020), ozone sondes measurements (Wohlmann et al., 2020), and chemical reanalyses by the CAMS (Inness et al., 2020). The minimum ozone column occurred in the first half of March, with March and April 2020 corresponding to the lowest ozone recorded for the period 1979–2020.

The anomalies in the June monthly mean  $\text{NO}_x$  concentrations relative to climatology (Figure S5), resulting from interannual variations in atmospheric circulation and temperature, lightning-related  $\text{NO}_x$  formation and wildfire-related emissions (Case 4 = Control – CLIMO), reaches up to 25%. This magnitude is comparable to, or even higher than, the effect generated by the COVID-19 related emission reductions (up to –20%; see Case 3 = COVID-ALL – Control). Based on the “meteorological” model estimates (panel a), Case 4 = Control – CLIMO,  $\text{NO}_x$  should have been abnormally abundant in the free troposphere during 2020, particularly in the northern hemisphere. However, the perturbations in emissions due to the pandemic substantially reduced the  $\text{NO}_x$  level in northern hemisphere and tropics (panel b), Case 5 = COVID-ALL – CLIMO).

Poleward of 45°N, the anomaly in the zonally and monthly mean free tropospheric ozone concentration relative to the 19-yr climatology is influenced substantially by the pronounced springtime Arctic ozone depletion in the first months of 2020 (Case 4 = Control – CLIMO, panel c of Figure S5). This anomaly persisted between 400 and 20 hPa, poleward of 60°N, as late as June, although with a considerably lower

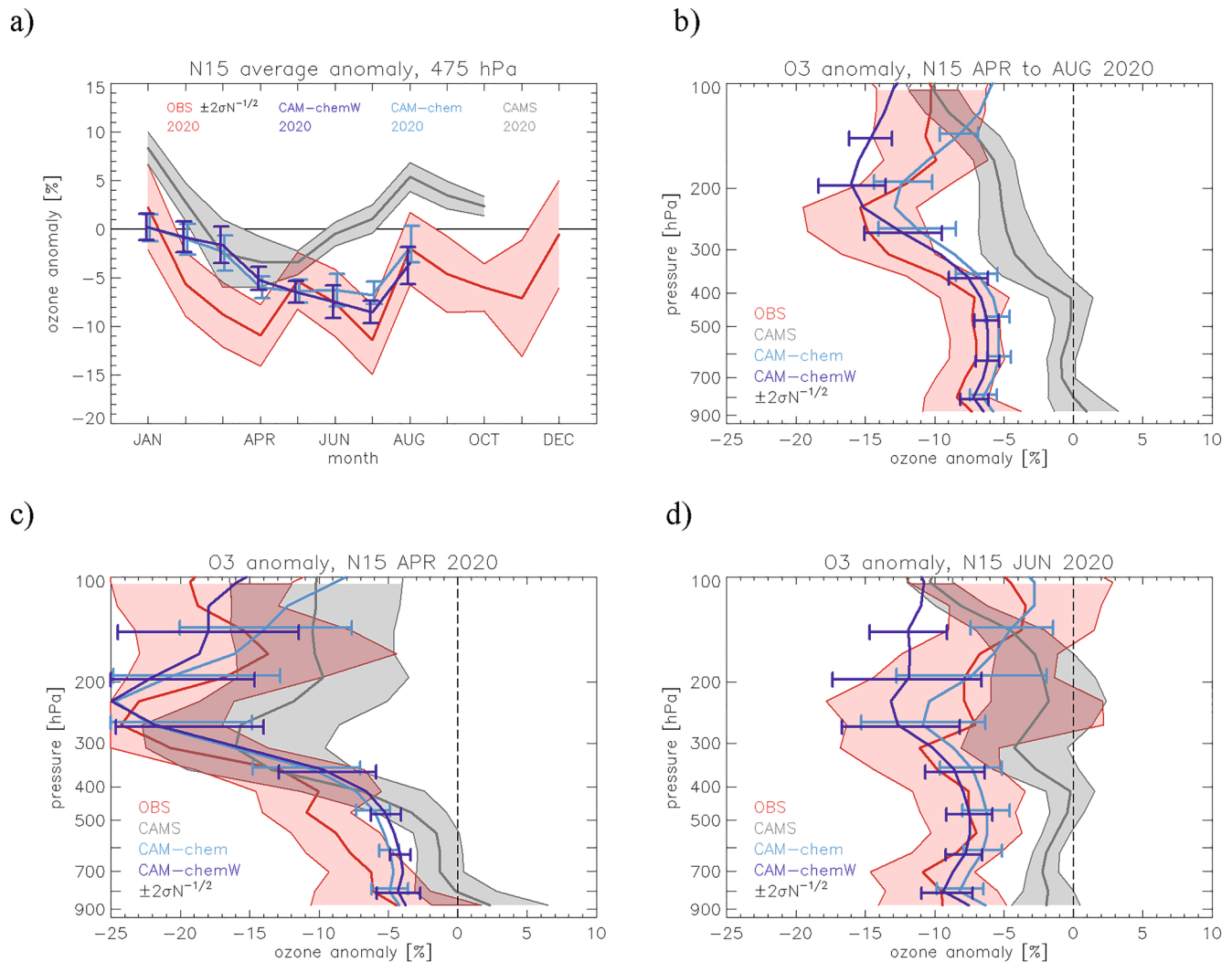


**Figure 3.** Panel (a) Annual course of 2020 ozone anomalies at 6 km altitude ( $\sim 420$  hPa), averaged over stations north of  $15^\circ\text{N}$ , as in Steinbrecht et al. (2021). Red: observations (Case 5). Light and dark blue: CAM-chem simulation (Case 5 = COVID-ALL – CLIMO), and CAM-chemW simulation (Case 6 = COVID-ALL2 – CLIMO) with larger Arctic stratospheric spring-time ozone depletion following Wilka et al. (2021). Gray: CAMS simulation (corresponding to Case 4 = Control – CLIMO). Panels (b–d): Profiles of the 2020 mean anomaly over stations north of  $15^\circ\text{N}$  for April–August, April, and June. Error bars and shading give  $\pm 2$  standard deviations of the mean over stations.

amplitude. The ozone concentration anomaly resulting from the perturbed emissions during the COVID-19 pandemic combined with the interannual variability ranged from 5% to 15% north of  $30^\circ\text{N}$  (Case 5 = COVID-ALL – CLIMO, panel d of Figure S5). Averaged vertical profiles of the anomalies are provided in Figure S6 (polar latitudes) and Figure S7 (hemispheric and tropical averages).

It is interesting to note that meteorologically induced positive ozone anomalies everywhere south of  $30^\circ\text{N}$  in 2020 (panel c of Figure S5, Case 4 = Control – CLIMO) appear to have masked the COVID-19 related ozone reductions in this region (see Figures 1 and 2, Case 3 = COVID-ALL – Control). The net ozone anomaly in 2020 was therefore small south of  $30^\circ\text{N}$  (panel d of Figure S5, Case 5 = COVID-ALL – CLIMO). This is consistent with the lack of large negative anomalies derived from the observations in the tropics and in the Southern Hemisphere (Steinbrecht et al., 2021; Figures S8, S10, and S11).

For the northern hemisphere, the comparison between our simulations (Case 5 = COVID-ALL – CLIMO) and the observations of Steinbrecht et al. (2021) is shown in Figure 3. Ozone monthly mean anomalies in the year 2020 were observed at about 45 locations worldwide (see Figure S8 for a map of the locations), and are averaged here over all stations north of  $15^\circ\text{N}$ . Figure 3 also shows corresponding anomalies simulated

by the CAMS. The CAMS simulations account for 2020 meteorological conditions (including the large stratospheric ozone depletion in the Arctic), but do not include effects of the reduced emissions due to the COVID-19 pandemic in 2020 (Case 4). Panel a of Figure 3 shows the resulting annual courses of ozone anomalies at 6 km altitude ( $\sim 420$  hPa), averaged over all northern extratropical stations (stations north of  $15^\circ\text{N}$ ). All data sets show increasingly negative anomalies from January to April 2020, largely due to 2020 meteorological conditions and Arctic stratospheric ozone depletion in 2020 (compare Figure S5). Observations and CAMS show similar decline from January to April; the CAM-chem simulations (Case 5 = COVID-ALL – CLIMO) give less of a decline. From April onwards, photochemical ozone production becomes increasingly important, and the reduced emissions of 2020 play a major role (compare Figures 1 and S7). Consequently, observations and CAM-chem simulations show persistent negative anomalies (Case 5) of  $-5\%$  to  $-10\%$ . Panels b–d in Figure 3 shows vertical profiles of the ozone anomaly, averaged over the 4 months from April to August 2020, and for the single months April and June.

To assess uncertainties for the influence of the large Arctic spring-time stratospheric ozone depletion, a sensitivity test was performed with the CAM-chem model (Case 6): According to the suggestion of Wilka et al. (2021), larger number densities of nitric acid trihydrate particles ( $10^{-5} \text{ cm}^{-3}$ ) were assumed in the Arctic lower stratosphere (Case 6, scenario CAM-chemW). This increases the denitrification rate in these layers and hence increases the catalytic destruction of ozone by active chlorine. When they adopted these conditions, Wilka et al. (2021) found better agreement between the calculated and observed nitric acid and ozone concentrations. This scenario provides an upper bound for the stratospheric ozone reduction (Case 6, CAM-Chem-W, dark blue line) and gives about 1% more ozone reduction in the troposphere from May to August. It is generally in better agreement with the observations (red lines and shaded area, see also panels b–d)). In contrast to observations and both CAM-chem simulations (Cases 5 and 6 = COVID-ALL(2) – CLIMO), CAMS (no emission reductions, Case 4, gray lines and shading) simulates increasing ozone from May onwards. By July, CAMS simulates anomalies near or above zero. The good agreement between observations and CAM-chem simulations (cases 5 and 6 = COVID-ALL(2) – CLIMO) from April to August, and their difference with respect to CAMS (Case 4, no emission reductions), further confirms that the negative ozone anomaly of  $-5\%$  to  $-10\%$  in late spring and summer 2020 was caused largely by reduced emissions, with some influence from the 2020 Arctic spring-time depletion of stratospheric ozone.

## 5. Uncertainties

As stated above, the model simulations have been performed by adopting the central values (best estimates) of the CONFORM adjustment factors (Doumbia et al., 2021). These factors are subject to uncertainties ranging typically from 10% to 25% depending on the economic sector and the region of the world (see Table S1). These uncertainties translate into errors of the same order of magnitude on the calculated changes in the concentration of primary species. As the photochemistry of secondary species such as ozone is nonlinear, the response of these species to reduced emissions is expected to vary with the local photochemical environment, and should be quantified by an ensemble of model simulations that considers the uncertainties in the emissions for each economic sector. For example, when considering the uncertainty associated only with the reduction in aviation activity, the error in the calculated ozone reduction near 250 hPa is close to 1 ppbv. A complete estimate of the error in the calculated response of atmospheric constituents should also account for the differences in model formulations, which can also lead to substantial differences in the calculated responses.

## 6. Summary

The ozone abundance in the extratropical northern hemisphere free troposphere during spring and summer of 2020 has been 5%–15% lower than climatology. Assuming realistic scenarios, the ozone response to decreased emissions of primary pollutants associated with the reduction in economic activity including air-traffic during the COVID-19 pandemic is estimated to be 4%–8%. Reduced worldwide aircraft operations had the highest impact in the middle and upper troposphere of the northern hemisphere during the summer months. The impact of 2020 meteorological conditions and the abnormally high ozone depletion in the Arctic lower stratosphere during the spring and summer of 2020 also produces a noticeable ozone



reduction of 3%–10% in the northern extratropical free troposphere. This effect is noticeable until late spring and reaches a maximum in June. Below 400 hPa, however, the influence of the stratosphere remains small, compared to the effect of the COVID-19-related reduction. For regions south of 30°N, the tropics and the southern hemisphere, the simulations indicate that a 4%–6% reduction of ozone due to COVID-19 related emission reductions did take place in 2020, but was largely compensated by ozone (and nitrogen oxides) increases caused by the specific meteorological conditions of 2020.

Our study has estimated the response of free tropospheric ozone to an unprecedented real reduction in global anthropogenic emissions. The model simulations successfully reproduce the observed ozone anomalies in the free troposphere during the 6 months that followed the COVID-19 outbreak. They provide a quantitative estimate of the different factors that contributed to the observed ozone anomalies. We also tested the sensitivity of our results to enhanced spring-time ozone destruction in the Arctic stratosphere, and to a more moderate reduction of aircraft emissions during the COVID-19 crisis. While these changes have some effect, they do not fundamentally alter our conclusions. Overall, our different tested scenarios, together with similar ozone reductions obtained in other simulations (Mertens et al., 2021; Miyazaki et al., 2021; Weber et al., 2020) indicate that the uncertainty of the calculated ozone anomaly in the free troposphere is of the order of 1–2 ppbv (2%–4%), and is associated with the adopted model formulation as well as the assumed magnitude of the emission reductions. As more accurate information on actual emission reductions becomes available, future simulations should reduce the current uncertainties. Clearly, global and regional air quality forecast and reanalysis models are now starting to account better for the disturbances, which occurred in the atmospheric chemical system due to reduced emissions under the COVID-19 pandemic after January 2020.

## Data Availability Statement

CESM2.2.0 is a publicly released version of the Community Earth System Model and freely available online at <https://zenodo.org/record/3895315>. The results of the model simulations are available online (Gaubert et al., 2021, <https://doi.org/10.5065/cgg0-rr19>). The CAMS-GLOB-ANT\_V4.2\_R1.1 surface emissions and the CONFORM adjustment factors are publicly available from the ECCAD database (<https://eccad.aeris-data.fr/essd-conform>).

## References

- Archibald, A. T., Neu, J. L., Elshorbany, Y. F., Cooper, O. R., Young, P. J., Akiyoshi, H., et al. (2020). Tropospheric Ozone Assessment Report: A critical review of changes in the tropospheric ozone burden and budget from 1850 to 2100. *Elementa, Science of the Anthropocene*, 8(1), 034. <https://doi.org/10.1525/elementa.2020.034>
- Bates, K. H., & Jacob, D. J. (2020). An expanded definition of the odd oxygen family for tropospheric ozone budgets: Implications for ozone lifetime and stratospheric influence. *Geophysical Research Letters*, 47(4), e2019GL084486. <https://doi.org/10.1029/2019GL084486>
- Bauwens, M., Compennolle, S., Stavrou, T., Müller, J.-F., van Gent, J., Eskes, H., et al. (2020). Impact of coronavirus outbreak on NO<sub>2</sub> pollution assessed using TROPOMI and OMI observations. *Geophysical Research Letters*, 47, e2020GL087978. <https://doi.org/10.1029/2020GL087978>
- Cazorla, M., Herrera, E., Palomeque, E., & Saud, N. (2020). What the COVID-19 lockdown revealed about photochemistry and ozone production in Quito, Ecuador. *Atmospheric Pollution Research*, 12, 124–133. <https://doi.org/10.1016/j.apr.2020.08.028>
- Danabasoglu, G., Lamarque, J.-F., Bacmeister, J., Bailey, D. A., DuVivier, A. K., Edwards, J., et al. (2020). The Community Earth System Model version 2 (CESM2). *Journal of Advances in Modeling Earth Systems*, 12, e2019MS001916. <https://doi.org/10.1029/2019MS001916>
- Darmenov, A., & da Silva, A. M. (2014). *The QuickFire emissions dataset (QFED)—Documentation of versions 2.1, 2.2 and 2.4, NA-SATM-2013-104606* (Vol. 35, p. 183). Retrieved from <https://portal.nccs.nasa.gov/datashare/ies/aerosol/emissions/QFED/v2.4r6/>
- Deroubaix, A., Brasseur, G., Gaubert, B., Labuhn, I., Menut, L., Siour, G., & Tuccella, P. (2021). Response of surface ozone concentration to emission reduction and meteorology during the COVID-19 lockdown in Europe. *Meteorological Applications*, 28(3), e1990. <https://doi.org/10.1002/met.1990>
- Doumbia, T., Granier, C., Elguindi, N., Bouarar, I., Darras, S., Brasseur, G., et al. (2021). Changes in global air pollutant emissions during the COVID-19 pandemic: A dataset for atmospheric chemistry modeling. *Earth System Science Data Discussion*. [Preprint]. <https://doi.org/10.5194/essd-2020-348>
- Elguindi, N., Granier, C., Stavrou, T., Darras, S., Bauwens, M., Cao, H., et al. (2020). Intercomparison of magnitudes and trends in anthropogenic surface emissions from bottom-up inventories, top-down estimates, and emission scenarios. *Earth's Future*, 8, e2020EF001520. <https://doi.org/10.1029/2020EF001520>
- Emmons, L. K., Schwantes, R. H., Orlando, J. J., Tyndall, G., Kinnison, D., Lamarque, J.-F., et al. (2020). The Chemistry Mechanism in the Community Earth System Model version 2 (CESM2). *Journal of Advances in Modeling Earth Systems*, 12, e2019MS001882. <https://doi.org/10.1029/2019MS001882>
- Gaubert, B., Bouarar, I., Doumbia, T., Liu, Y., Stavrou, T., Deroubaix, A., et al. (2021). Global changes in secondary atmospheric pollutants during the 2020 COVID-19 pandemic. *Journal of Geophysical Research: Atmospheres*, 126, e2020JD034213. <https://doi.org/10.1029/2020JD034213>

## Acknowledgments

We would like to acknowledge the high-performance computing support from Cheyenne (<https://doi.org/10.5065/D6RX99HX>) provided by NCAR's Computational and Information Systems Laboratory of the National Center for Atmospheric Research (NCAR), sponsored by the US National Science Foundation (NSF). This material is based upon work supported by the National Center for Atmospheric Research, which is a major facility sponsored by the National Science Foundation under cooperative agreement no. 1852977. We also acknowledge the support of the AQ-WATCH European project, a HORIZON 2020 Research and Innovation Action (GA 870301). The surface emissions adopted in the present study are based on the CAMS-GLOB-ANT dataset that has been developed with the support of the CAMS (Copernicus Atmosphere Monitoring Service), operated by the European Center for Medium-Range Weather Forecasts on behalf of the European Commission as part of the Copernicus Programme. Tao Wang and Yiming Liu acknowledge support by the Hong Kong Research Grants Council (T24-504/17-N and A-PolyU502/16). Trisseyeni Stavrou acknowledges the support of the ICovac and TROVA projects funded by ESA. Open access funding enabled and organized by Projekt DEAL.

- Gaubert, B., Emmons, L. K., Reader, K., Tilmes, S., Miyazaki, K., Arellano, A. F. Jr., et al. (2020). Correcting model biases of CO in East Asia: Impact on oxidant distributions during KORUS-AQ. *Atmospheric Chemistry and Physics*, 20, 14617–14647. <https://doi.org/10.5194/acp-20-14617-2020>
- Gaubert, B., Tilmes, S., Bouarar, I., Doumbia, T., Liu, Y., Stavrou, T., et al. (2020). CAM-chem simulation of the 2020 lockdown. Version 3.0. UCAR/NCAR—DASH Repository. <https://doi.org/10.5065/cgg0-rr19>
- Gelaro, R., McCarty, W., Suarez, M. J., Molod, A., Takacs, L., Randles, C. A., et al. (2017). The Modern-Era Retrospective Analysis for Research and Applications, version 2 (MERRA-2). *Journal of Climate*, 30(14), 5419–5454. <https://doi.org/10.1175/JCLI-D-16-0758.1>
- Gettelman, A., Mills, M. J., Kinnison, D. E., Garcia, R. R., Smith, A. K., Marsh, D. R., et al. (2019). The whole atmosphere community climate model version 6 (WACCM6). *Journal of Geophysical Research: Atmospheres*, 124, 12380–12403. <https://doi.org/10.1029/2019JD030943>
- Goldberg, D. L., Vinciguerra, T. P., Hosley, K. M., Loughner, C. P., Canty, T. P., Salawitch, R., & Dickerson, R. R. (2015). Evidence for an increase in the ozone photochemical lifetime in the eastern United States using a regional air quality model. *Journal of Geophysical Research*, 120(24), 12778–12793. <https://doi.org/10.1002/2015JD023930>
- Granier, C., Darras, S., Denier van der Gon, H., Doubalova, J., Elguindi, N., Galle, B., et al. (2019). The Copernicus atmosphere monitoring service global and regional emissions. [Research report]. Copernicus Atmosphere Monitoring Service (CAMS). <https://doi.org/10.24380/d0bn-kx16>
- Guenther, A. B., Jiang, X., Heald, C. L., Sakulyanontvittaya, T., Duhl, T., Emmons, L. K., & Wang, X. (2012). The Model of Emissions of Gases and Aerosols from Nature version 2.1 (MEGAN2.1): An extended and updated framework for modeling biogenic emissions. *Geoscientific Model Development*, 5, 1471–1492. <https://doi.org/10.5194/gmd-5-1471-2012>
- Hoesly, R. M., Smith, S. J., Feng, L., Klimont, Z., Janssens-Maenhout, G., Pitkanen, T., et al. (2018). Historical (1750–2014) anthropogenic emissions of reactive gases and aerosols from the Community Emissions Data System (CEDS). *Geosciences Model Development*, 11, 369–408. <https://doi.org/10.5194/gmd-11-369-2018>
- Huang, X., Ding, A., Gao, J., Zheng, B., Zhou, D., Qi, X., et al. (2020). Enhanced secondary pollution offset reduction of primary emissions during COVID-19 lockdown in China. *National Science Review*, 8, 1–9. <https://doi.org/10.1093/nsr/nwaa137>
- Inness, A., Chabrilat, S., Flemming, J., Huijnen, V., Langenrock, B., Nicolas, J., et al. (2020). Exceptionally low Arctic stratospheric ozone in spring 2020 as seen in the CAMS reanalysis. *Journal of Geophysical Research: Atmospheres*, 125, e2020JD033563. <https://doi.org/10.1029/2020JD033563>
- Lamboll, R. D., Jones, C. D., Skeie, R. B., Fiedler, S., Samsey, B. H., Gillett, N. P., et al. (2021). Modifying emissions scenario projections to account for the effects of COVID-19: Protocol for CovidMIP. *Geoscientific Model Development*, 14, 3683–3695. <https://doi.org/10.5194/gmd-14-3683-2021>
- Lawrence, D. M., Fisher, R. A., Koven, C. D., Oleson, K. W., Swenson, S. C., Bonan, G., et al. (2019). The Community Land Model version 5: Description of new features, benchmarking, and impact of forcing uncertainty. *Journal of Advances in Modeling Earth Systems*, 11, 4245–4287. <https://doi.org/10.1029/2018MS001583>
- Le, T., Wang, Y., Liu, L., Yang, J., Yung, Y. L., Li, G., & Seinfeld, J. H. (2020). Unexpected air pollution with marked emission reduction during the COVID-19 outbreak in China. *Science*, 369, 702–706. <https://doi.org/10.1126/science.abb7431>
- Lian, X., Huang, J., Huang, R., Liu, C., Wang, L., & Zhang, T. (2020). Impact of city lockdown on the air quality of COVID-19-hit of Wuhan city. *The Science of the Total Environment*, 742, 140556. <https://doi.org/10.1016/j.scitotenv.2020.140556>
- Liu, X., Ma, P.-L., Wang, H., Tilmes, S., Singh, B., Easter, R. C., et al. (2016). Description and evaluation of a new four-mode version of the Modal Aerosol Module (MAM4) within version 5.3 of the Community Atmosphere Model. *Geoscientific Model Development*, 9(2), 505–522. <https://doi.org/10.5194/gmd-9-505-2016>
- Liu, Y., Wang, T., Stavrou, T., Elguindi, N., Doumbia, T., Granier, C., et al. (2021). Diverse response of atmospheric ozone to COVID-19 lockdown in China. *Science of the Total Environment*, 789, 147739. <https://doi.org/10.1016/j.scitotenv.2021.147739>
- Manney, G. L., Livesey, N. J., Santee, M. L., Froidevaux, L., Lambert, A., Lawrence, Z. D., et al. (2020). Record-low Arctic stratospheric ozone in 2020: MLS observations of chemical processes and comparisons with previous extreme winters. *Geophysical Research Letters*, 47, e2020GL089063. <https://doi.org/10.1029/2020GL089063>
- Mertens, M., Jöckel, P., Mathes, S., Nützel, M., Grewe, M., & Sausen, R. (2021). COVID-19 induced lower tropospheric ozone changes. *Environmental Research Letters*, 16, 064005. <https://doi.org/10.1088/1748-9326/abf191>
- Mills, M. J., Schmidt, A., Easter, R., Solomon, S., Kinnison, D. E., Ghan, S. J., et al. (2016). Global volcanic aerosol properties derived from emissions, 1990–2014, using CESM1 (WACCM). *Journal of Geophysical Research: Atmospheres*, 121, 2332–2348. <https://doi.org/10.1002/2015JD024290>
- Miyazaki, K., Bowman, K., Sekiya, T., Jiang, Z., Chen, X., Eskes, H., et al. (2020). Air quality response in China linked to the 2019 novel coronavirus (COVID-19) lockdown. *Geophysical Research Letters*, 47, e2020GL089252. <https://doi.org/10.1029/2020gl089252>
- Miyazaki, K., Bowman, K., Sekiya, T., Takigawa, M., Neu, J. L., Sudo, K., et al. (2021). Global tropospheric ozone responses to reduced NOx emissions linked to the COVID-19 worldwide lockdowns. *Science Advances*, 7, eabf7460. <https://doi.org/10.1126/sciadv.abf7460>
- Ordóñez, C., Garrido-Perez, J. M., & García-Herrera, R. (2020). Early spring near-surface ozone in Europe during the COVID-19 shutdown: Meteorological effects outweigh emission changes. *The Science of the Total Environment*, 747, 141322. <https://doi.org/10.1016/j.scitotenv.2020.141322>
- Schumann, U., Bugliaro, L., Dörnbrack, A., Baumann, R., & Voigt, C. (2021). Aviation contrail cirrus and radiative forcing over Europe during 6 months of COVID-19. *Geophysical Research Letters*, 48, e2021GL092771. <https://doi.org/10.1029/2021gl092771>
- Shi, X., & Brasseur, G. P. (2020). The response in air quality to the reduction of Chinese economic activities during the COVID-19 outbreak. *Geophysical Research Letters*, 47, e2020GL088070. <https://doi.org/10.1029/2020GL088070>
- Steinbrecht, W., Kubistin, D., Plass-Dülmer, C., Davies, J., Tarasick, D. W., Gathen, P., et al. (2021). COVID-19 crisis reduces free tropospheric ozone across the Northern Hemisphere. *Geophysical Research Letters*, 48, e2020GL091987. <https://doi.org/10.1029/2020GL091987>
- Stevenson, D. S., Dentener, F. J., Schultz, M. G., Ellingsen, K., van Noije, T. P. C., Wild, O., et al. (2006). Multimodel ensemble simulations of present-day and near-future tropospheric ozone. *Journal of Geophysical Research*, 111, D08301. <https://doi.org/10.1029/2005JD006338>
- Terao, Y., Logan, J. A., Douglass, A. R., & Stolarski, R. S. (2008). Contribution of stratospheric ozone to the interannual variability of tropospheric ozone in the northern extratropics. *Journal of Geophysical Research*, 113, D18309. <https://doi.org/10.1029/2008JD009854>
- Tilmes, S., Hodzic, A., Emmons, L. K., Mills, M. J., Gettelman, A., Kinnison, D. E., et al. (2020). Climate forcing and trends of organic aerosols in the Community Earth System Model (CESM2). *Journal of Advances in Modeling Earth Systems*, 11, 4323–4351. <https://doi.org/10.1029/2019MS001827>
- Venter, Z. S., Aunan, K., Chowdhury, S., & Lelieveld, J. (2020). COVID-19 lockdowns cause global air pollution declines. *Proceedings of the National Academy of Sciences of the United States of America*, 117(32), 18984–18990. <https://doi.org/10.1073/pnas.2006853117>

- Weber, J., Shin, Y. M., Staunton Sykes, J., Archer-Nicholls, S., Abraham, N. L., & Archibald, A. T. (2020). Minimal climate impacts from short-lived climate forcers following emission reductions related to the COVID-19 pandemic. *Geophysical Research Letters*, 47, e2020GL090326. <https://doi.org/10.1029/2020GL090326>
- Wilka, C., Solomon, S., Kinnison, D., & Tarasick, D. (2021). An Arctic ozone hole in 2020 if not for the Montreal protocol. *Atmospheric Chemistry and Physics Discussion*. <https://doi.org/10.5194/acp-2020-1297>
- Wohlmann, I., von der Gathen, P., Lehmann, R., Maturilli, M., Deckelmann, H., Manney, G. L., et al. (2020). Near-complete local reduction of Arctic stratospheric ozone by severe chemical loss in spring 2020. *Geophysical Research Letters*, 47, e2020GL089547. <https://doi.org/10.1029/2020GL089547>